Accepted manuscript; © IEEE Journal of Photovoltaics; final version available at 10.1109/JPHOTOV.2017.2777667

Extracting Nonradiative Parameters in III-V Semiconductors using Double-Heterostructures on Active *p-n* Junctions

A. W. Walker, J. Schön, F. Dimroth

Fraunhofer Institute for Solar Energy Systems ISE, Heidenhofstraße 2, 79110 Freiburg

***Abstract*—A novel method of extracting the nonradiative lifetime of $Ga_{0.51}In_{0.49}P$ lattice matched to GaAs by exploiting luminescence coupling is discussed. The method requires a GaInP double-heterostructure monolithically grown on a GaAs photodetector for quantum efficiency measurements. The method then extracts the nonradiative lifetime by modeling the luminescence coupling between the GaInP and the GaAs active region. The bulk nonradiative lifetime of disordered GaInP doped to 10^{17} cm^{-3} under low level injection (~4×10^{12} cm^{-3}) is determined to be 47 ns for GaInP layer thicknesses ranging from 200 nm to 1500 nm, with a surface recombination velocity of 660 cm/s. The results are in agreement with nonradiative lifetimes extracted using power-dependent relative photoluminescence measurements, whereby the lifetimes increase as a function of injection level to 0.5 μs. Surface recombination velocities are also reported as a function of injection level using this technique, decreasing from 1800 cm/s under low injection to 50 cm/s under high injection (~10^{17} cm^{-3}). Lastly, the effective radiative lifetimes (accounting for photon recycling) are also reported for the studied GaInP samples.**

***Index Terms*—III-V semiconductors, luminescence coupling, radiative lifetime, modeling and simulation.**

I. Introduction

Minority carrier lifetimes and transport in III-V semiconductors with direct bandgaps are crucial in the performance of optoelectronic devices including light emitting diodes, photodetectors, lasers and solar cells. The recombination lifetime can be separated into a nonradiative component and a radiative component, both of which will depend on the injection level [1-2]. Ultimately, the nonradiative recombination lifetime via the Shockley-Read-Hall (SRH) process strongly depends on the quality of the crystalline material in terms of the concentration of defects, which depends primarily on the growth conditions; note that the concentration of dopants can also influence the concentration of defects above some reference doping level [3-4]. The radiative lifetime, on the other hand, is inherently linked to the radiative recombination coefficient, Brad and the doping concentration. The coefficient Brad is usually interpreted as a device parameter which depends on the properties of the optical system including absorption coefficient, layer thickness and the rear-side reflectivity, all of which influence photon recycling [1, 5]. It is also commonly referred to as the Einstein coefficient for spontaneous emission, i.e. a material parameter. When modeling an optoelectronic device such as a solar cell, the Einstein coefficient must be weighted by the optical influences of the system in terms of a photon recycling factor [6, 7]. The value of the Einstein coefficient and the photon recycling factor then become fundamental in modeling and optimizing radiatively dominated solar cells such as state-of-the-art single junction GaInP or GaAs cells with rear-side mirrors which exploit photon recycling [8-11] as well as multi-junction solar cells, which are achieving 46% efficiency under concentrated illumination [12].

The effective minority carrier lifetimes of direct semiconductors, given by the radiative and nonradiative terms combined, are commonly measured using time-resolved photoluminescence (TRPL). This technique has also been used to extract the nonradiative component of the effective carrier lifetime and the radiative recombination coefficient by exploiting their respective carrier concentration dependencies under a particular injection level [5]. Note that with this method (and in all photoluminescence based experiments), the radiative recombination coefficient should be interpreted as a device parameter due to its dependence on the optical properties of the system. To extract both the radiative and nonradiative terms, several samples of different carrier concentrations must be evaluated, which requires considerable time, expertise and cost, considering the level of sophistication and calibration of a sub-nanosecond time scale measurement method. We propose a different method based on double-heterostructures (DHs) grown on a lower bandgap p-n junction (see Fig. 1), which gauges the magnitude of the luminescence coupling between the DH and the *p-n* junction via quantum efficiency (QE) measurements. Double-heterostructures are standard in the development of multi-junction solar cells for photoluminescence-based measurements, so the inclusion of a monolithic *p-n* junction directly below the DH is rather straightforward. Furthermore, knowledge of the optical parameters and QE measurements are the only data input necessary to extract the nonradiative lifetime at a particular injection level using the proposed method. Note that a device model capable of accounting for luminescence coupling between two adjacent regions is required. As a comparison and justification, the results from this proposed method are compared to nonradiative lifetimes extracted using power-

ARC		
30 nm	p-AlGaInP:Zn barrier	2.0E18 cm^{-3}
X nm	p-GaInP:Zn test layer	1.0E17 cm^{-3}
30 nm	p-AlGaInP:Zn barrier	2.0E18 cm^{-3}
180 nm	p-GaAs:Zn emitter	1.0E18 cm^{-3}
2000 nm	n-GaAs:Se base	1.0E17 cm^{-3}
50 nm	n-GaInP:Se barrier	2.0E18 cm^{-3}
500 nm	n-GaAs:Se buffer	1.0E18 cm^{-3}
450 μm	n-GaAs:Se substrate	1.0E18 cm^{-3}

Figure 1. Structural details of lattice matched GaInP double-heterostructures cladded with AlGaInP and grown on a GaAs *p-n* junction on GaAs substrate. The thickness of the GaInP layer, *X*, ranges from 200 nm to 1500 nm.

dependent photoluminescence measurements [1].

In this paper, the nonradiative lifetime of disordered $Ga_{0.51}In_{0.49}P$ (hereafter GaInP) lattice matched to GaAs is extracted using the device modeling of DH test structures stacked on a GaAs photodetector. The adopted numerical model is based on a previously calibrated model which accounts for photon recycling [13], and has been generalized to account for luminescence coupling between two active, absorbing semiconductor regions [14]. The calibration of the model to the measured quantum efficiency characteristics of the structure thus reveals the nonradiative lifetime of the GaInP material. The paper is organized as follows. Section II outlines the structural details of the GaInP DHs of interest, followed by the experimental quantum efficiencies as a function of injection level. Section III introduces the modeling, including the discussion and interpretation of the radiative recombination coefficient B_{rad} and the calibration of the model to extract the nonradiative lifetime of GaInP in terms of both bulk and interface components. Section IV then compares these extracted lifetimes to results from power-dependent relative photoluminescence measurements. Section V finally gives the conclusions of the present study.

II. Structural Details & Experimental Results

Figure 1 illustrates the test structure of interest, whereby a preferentially disordered GaInP layer (with a bandgap close to 1.9 eV) is cladded by $(Al_{0.6}Ga_{0.4})_{0.51}In_{0.49}P$ barrier layers and grown on a *p-n* junction composed of GaAs. This GaAs *p-n* junction is composed of a 120 nm thick 10^{18} cm^{-3} doped emitter, and a 2.0 μm thick 10^{17} cm^{-3} *p*-type base. These structures were realized using metal-organic vapor phase epitaxy on 4" GaAs (100) substrates with a 6° offcut toward the <111>B direction. Three different thicknesses of the GaInP DH are explored: 200, 700 and 1500 nm all nominally

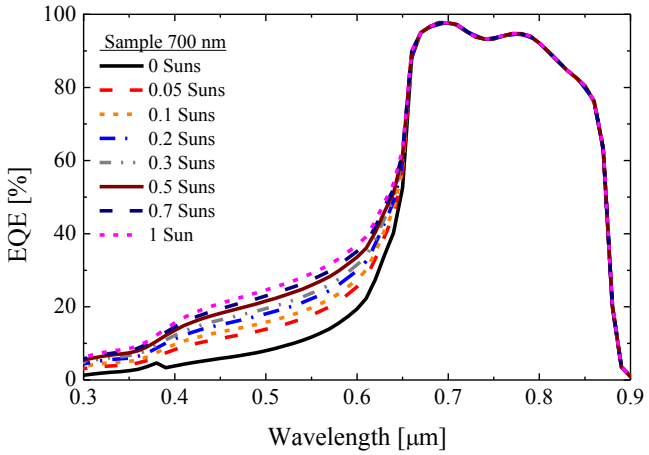

Figure 2. Measured external quantum efficiency of a 700 nm GaInP DH on a GaAs *p-n* junction for increasing white light bias intensity expressed in suns (1 sun corresponds to 1000 W/m^2 based on a calibrated silicon cell).

doped to 10^{17} cm^{-3}. An anti-reflection coating (ARC) composed of Ta_2O_5/MgF_2 is deposited on the front AlGaInP barrier layer to reduce incident reflectivity. Standard photolithography and mesa-etching are used to process the final 4 cm^2 solar cell devices.

The measured quantum efficiency for a 700 nm thick GaInP DH (sample C1136) is shown in Figure 2 for increasing white light bias intensity; the intensity of this bias light is given in suns based on a calibrated silicon reference cell. For no bias light intensity (i.e. the lowest injection level), there is a negligible amount of luminescence coupling from the GaInP absorber layer into the GaAs, and the signal between 300 and 650 nm is due to the transmission of photons through the GaInP DH. A sharp kink is visible in this particular signal at 380 nm since the monochromatic light source is changed from a Xe bulb to a Halogen bulb whereby the former is brighter (thus probing a slightly higher injection level). This kink disappears under non-zero bias light intensities since the white light source is significantly brighter than the monochromatic light sources (i.e. the Xe and Halogen bulbs). For wavelengths longer than 370-400 nm, there is an increased EQE due to less absorption occurring in the AlGaInP barrier layer. As the bias light intensity increases from 0 to 1 sun intensity, the measured EQE increases in magnitude as a result of stronger luminescence coupling from the GaInP DH into the GaAs. This increased coupling originates from the increased injection level, which increases the internal radiative efficiency η_{int} of GaInP, defined as the ratio of the radiative recombination rate to the total recombination rate, or

$$\eta_{\text{int}} = \frac{U_{\text{rad}}}{U_{\text{rad}}+U_{\text{srh}}+U_{\text{auger}}}, \qquad (1)$$

where U_{rad} is the radiative recombination rate, U_{srh} is the nonradiative Shockley-Read-Hall (SRH) recombination rate, and U_{auger} is the Auger recombination rate. An increase in η_{int} under these relatively low injection levels can be explained by a reduced nonradiative (SRH) recombination rate rather than

an increased radiative recombination rate. The low injection condition (or $\Delta n \ll N_A$) supports this explanation because the radiative lifetime (τ_{rad}), given by

$$\tau_{\rm rad} = {}^{1}\!\Big/\!_{B_{\rm rad}(N_{A,D}+\Delta n)}, \qquad (2)$$

remains fixed under low injection. Note that Auger is negligible under these low injection levels. Thus the increased luminescence coupling into the GaAs *p-n* junction as a function of bias light intensity can be explained by a trap saturation effect [2], which is an effect also observed in power-dependent relative photoluminescence experiments of GaAs DHs [1]. However, these EQE measurements do not yield quantitative insight into the internal radiative efficiency of the GaInP. Quantitative insight can be gained by numerical device modeling which accounts for photon recycling and luminescence coupling, as discussed in the next section.

III. Numerical Device Modeling

The modeling environment of TCAD Sentaurus vI-2013.12 (Synopsys, Mountain View, California, USA) is adopted to solve the semiconductor transport equations self-consistently using both finite-difference discretization methods. Details on the modeling environment can be found elsewhere, including the relevant material properties and the incorporation of photon recycling and luminescence coupling models [13-15]. Band offsets at heterointerfaces are adopted from [16]. However, the CBO at the $(Al_xGa_{1-x})InP/GaInP$ within the direct bandgap regime of AlGaInP (x<~0.5) is assumed to correspond to ~80% of the total reported CBO at the AlInP/GaInP interface because ~80% of the bandgap difference between GaInP and AlInP occurs in this molar fraction range. Prior to discussing the results of the simulation, however, a brief discussion on the radiative recombination coefficient must be given.

A. Radiative Recombination Coefficient

The radiative recombination coefficient of GaInP is critical in dictating the magnitude of the luminescence coupling to GaAs, since it dictates the magnitude of the isotropic radiative recombination rate occurring within the material. In the literature, this parameter is 10^{-10} cm^3s^{-1} according to Levinshtein for GaInP [17], which corresponds to a lifetime of 100 ns in a material with a doping concentration of 10_{17} cm_{-3}. However, since this value is experimental in nature, the thickness of the emitting material, as well as the optical properties of the system play an important role in determining this effective radiative recombination coefficient, primarily due to the influence of photon recycling. Care must therefore be taken in adopting a particular value of $B_{\rm rad}$ in modeling and simulation studies for III-V semiconductors such as GaAs or GaInP. For example, if one adopts a thermodynamic calculation for the isotropic radiative recombination coefficient [18], then it can be expressed as

$$B_{\rm rad} = \frac{1}{n_i^2}\frac{2\pi}{h^3c^2}\int_0^\infty \frac{n_S^2(E)\alpha(E)E^2}{e^{E/k_BT}-1}dE\ , \qquad (3)$$

where n_i is the intrinsic carrier concentration, $n_S(E)$ and $\alpha(E)$ are the refractive index and the absorption coefficient of the luminescing material respectively as a function of energy E, and the remaining parameters retain their usual meaning. Note that the absorption coefficient used in equation (3) must not account for below bandgap absorption due to defects, since the emission from such defect states is not observed experimentally at room temperature. The solution of equation (3) for the disordered GaInP material of interest with a bandgap close to 1.9 eV is 2.25×10^{-10} cm^3s^{-1}. This value of B_{rad} is more than twice the magnitude compared to the value from Levinshtein. Equation (3) does not account for any photon recycling effects and escape probabilities through the front surface, since it assumes isotropic emission which is independent of the optical properties of the system. Accounting for photon recycling effects requires more rigorous calculations [7, 13-14, 19]. In the adopted modeling and simulation environment of TCAD Sentaurus, isotropic radiative recombination is assumed, and the photon recycling is accounted for explicitly by relating the magnitude of the emission at each particular (mesh) point of the structure to all absorbing regions of the structure in a wavelength dependent manner [13-14]. Therefore, the value of 2.25×10^{-10} cm^3s^{-1} must be used in such numerical device simulations. For other device simulations which do not explicitly account for photon recycling, an effective B_{rad} value must be adopted which implicitly accounts for photon recycling using a photon recycling factor; see for example [7]. One should note, however, that luminescence coupling cannot be accounted for by using an effective B_{rad}.

B. Device Simulations

The nonradiative recombination lifetime of the GaInP material is extracted by calibrating the simulated external quantum efficiency (EQE) with photon recycling and luminescence coupling effects to the measured EQE of the structures. Note that the measured EQE must correspond to a particular white light bias intensity that gauges the same excess carrier concentration in each sample (see Figure 2). The AM1.5g has been assumed for the spectral shape of the white light source, which is found to be a reasonable approximation to the Halogen spectrum in estimating the carrier concentration in each sample. Based on the relative absorbance and thickness of each structure, as well as the minority carrier lifetime (extracted from the model calibration; see Figure 3), the white light bias intensities are ~0.7, ~0.5 and 1 sun (AM1.5g) for the 200, 700 and 1500 nm samples respectively. The model calibration is first performed in terms of the reflectivity based on layer thicknesses including the ARC, since the reflectivity is critical in fitting the measured EQE. Next, the wavelengths targeted for the GaAs *pn* junction are fitted based on nonradiative lifetimes in GaAs. The remaining parameter is essentially the nonradiative recombination lifetime of the GaInP, which is dependent on both bulk and interface effects. As a result, an effective SRH lifetime is adopted to account for both for each sample studied. Once the effective SRH lifetime is extracted, it can be

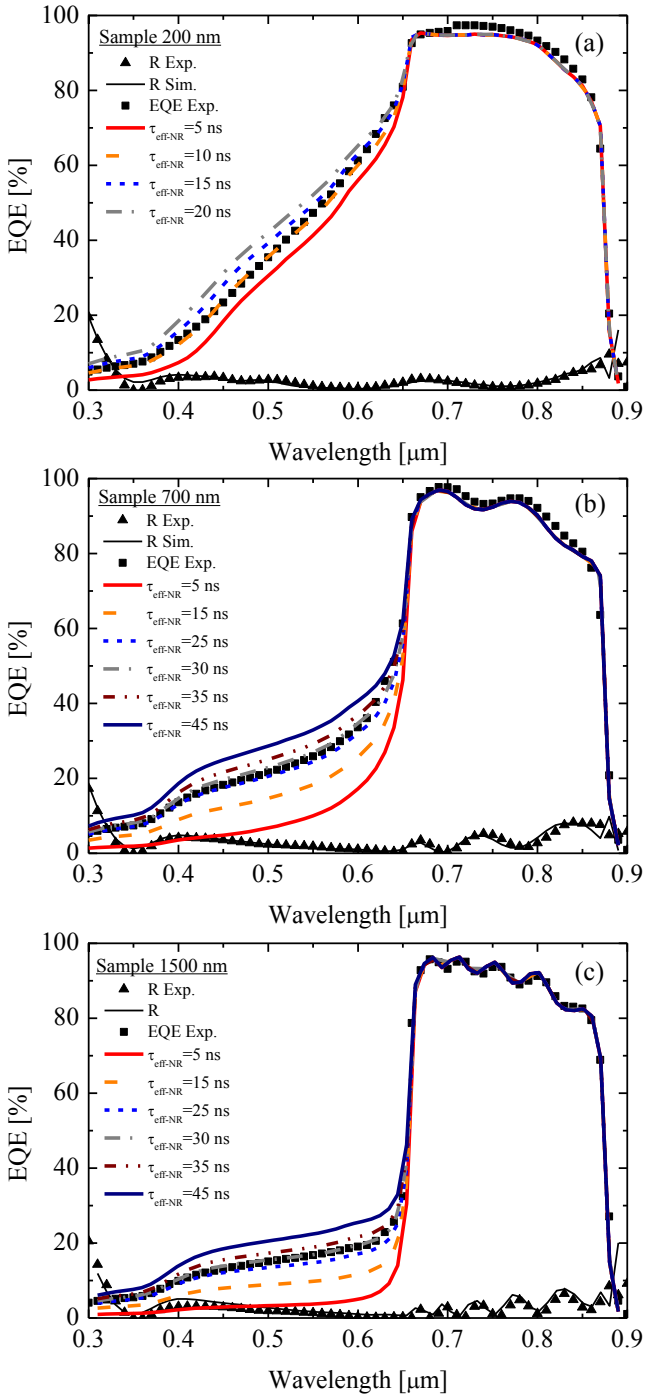

Figure 3. Simulated and experimental reflectivity and quantum efficiency of a) 200 nm GaInP DH, b) a 700 nm thick GaInP DH and a 1500 nmn GaInP DH for various effective nonradiative lifetimes. Experimental EQE curves correspond to 0.7 (a), 0.5 (b) and (c) 1 sun white light bias intensity respectively.

decoupled to extract the surface recombination velocity (SRV) for the GaInP/AlGaInP interfaces by fitting the dependence of the inverse effective nonradiative lifetime ($\tau_{\text{eff-NR}}$) as a function of inverse thickness (d) according to the relation

$$\frac{1}{\tau_{\text{eff-NR}}} = \frac{1}{\tau_{\text{srh}}} + \frac{2 \cdot SRV}{d}, \qquad (4)$$

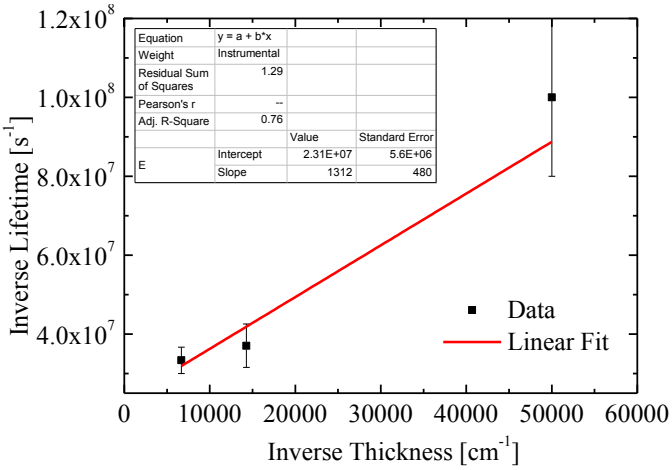

Figure 4. Best fit effective nonradiative lifetimes from Fig. 3 as a function of inverse thickness to extract the bulk and interface recombination parameters according to the best fit from equation (4).

where τ_{srh} is the bulk SRH recombination lifetime.

The simulated EQE results for each of the three samples are illustrated in Figure 3 for increasing effective SRH lifetimes; the scenario of no luminescence coupling is similar in magnitude to the 5 ns simulation and included to demonstrate the EQE signal due to the transparency of the GaInP layer. For example, the thinnest sample of 200 nm (Figure 3a) demonstrates the highest transparency compared to the other samples, or in other words, the highest EQE signal without luminescence coupling. As a result of this high transparency, this sample shows a relatively low impact of the luminescence coupling as the effective nonradiative lifetime is increased. The best-fit effective nonradiative lifetime is 10±2 ns; note the lifetime is based on the best-fit uncertainty as well as the uncertainty in probing the same excess carrier concentration. A SRH lifetime greater than 12 ns slightly over-estimates the EQE, thus hinting this value as an upper limit. Comparatively for the 700 nm sample, illustrated in Figure 3b, the overall transparency is reduced, which enables the coupling to be stronger, or in other words, a stronger dependence of the EQE signal on the nonradiative lifetime. The best-fit effective nonradiative lifetime for this sample is 27±4 ns, as seen in Figure 3b (the 30 ns simulation over-estimates the data). Again, the increased uncertainty for this sample is due to in part to the fitted data and in part to the higher uncertainty in the white light bias intensity. Lastly, the thickest sample of 1200 nm demonstrates the least transparency of all samples, and shows a comparable influence of increasing luminescence on the overall EQE as the 700 nm sample. The resulting best-fit effective nonradiative lifetime is 30±3 ns, as outlined in Figure 3c. In general, the results of Figure 3 show good agreement in both the reflectivity and the EQE in the GaAs wavelength range, and demonstrates a valid model for the optical constants.

The final step is to exploit the dependence of the effective nonradiative lifetime on thickness to extract the surface recombination velocity and bulk lifetime. The results are illustrated in Figure 4, and reveal a bulk SRH lifetime of

47±11 ns and a surface recombination velocity of 660±240 cm/s. The uncertainties have two origins: 1) the uncertainty of each extracted nonradiative lifetime based on the best-fit to the EQE, and 2) the uncertainty in white light bias intensity which probes each sample with the same excess carrier concentration; this includes the influence of the spectral shape of the bias light source as a function of intensity.

It is worth noting here that a previous study on the effective minority carrier lifetime in ordered *p*-GaInP demonstrated lifetimes as long as 29 ns, whereby a more disordered system resulted in lifetimes below 10 ns [20]. This outlines the high material quality of the disordered GaInP investigated here.

IV. Power-Dependent Relative Photoluminescence

The power-dependent relative PL (PDR-PL) measurement technique is a contactless photoluminescence method which relates the integrated photoluminescence of a sample to its maximum measured photoluminescence as a function of incident laser intensity [1]. The measurement gives direct insight into the effective radiative efficiency of the luminescing material, defined as the probability that an electron-hole pair will recombine radiatively and the resulting photon escapes the DH either via the front side into air, or the rear-side of the absorbing layer into the substrate. The effective radiative efficiency is identical to equation (1), with the exception that an effective radiative recombination is used to compute the radiative recombination rate, where this effective B_{rad} accounts implicitly for photon recycling and photon escape. In other words, the effective B_{rad} is not computed using equation (3), and more-so represents an experimental B_{rad}. Note that the effective radiative efficiency differs from both the external and internal radiative efficiency in that the external gauges the probability that the photoluminescence will escape the DH solely through the front surface, and the internal radiative efficiency gauges the probability that the electron-hole pair will recombine radiatively irrespective of the optical properties of the structure. As described in [1], extracting the effective radiative efficiency enables for the nonradiative parameter extraction of the SRH lifetime and the interface recombination velocity. Figure 5 illustrates the measured PDR-PL signal of each of the three GaInP DH samples where each point represents the integrated GaInP emission spectrum (see the inset plot) divided by the laser power, and the overall signal is subsequently normalized to the maximum. The normalization to unity represents a purely radiative material, or in other words a condition in which nonradiative recombination is negligible. In this case, the effective radiative efficiency is unity.

A. Measurement Results

For the 700 nm thick sample, the effective radiative efficiency increases from 13% to close to 32% as the laser intensity increases from 10 to 1000 W/m^2. The results are similar albeit lower for the thinnest (200 nm) sample, which indicates similar material quality at first sight. However, one would expect that, assuming similar bulk material quality between all samples, interface recombination would be strongest in the thinnest sample, and therefore the thinnest sample would show the lowest effective radiative efficiency. The missing link is that thinner samples experience less photon recycling due to less re-absorption, which is manifested by a shorter radiative lifetime [1]. Thus the effective radiative efficiency is expected to be higher for thinner structures. The fact that the thinnest structure does not show the highest radiative efficiency implies that interface recombination is playing an important role. The computed effective radiative recombination coefficients and corresponding radiative lifetimes which account for photon recycling and photon escape according to the model from reference [1] are summarized in Table I for all structures of interest. Note that as the GaInP DH thickness increases to 1500 nm, a reasonable agreement is reached with that given by Levinshtein of 10^{-10} cm^{3}s^{-1}. This re-iterates the dependence of the radiative recombination coefficient on thickness, and indicates a possible thickness range from which the Levinshtein data was extracted. With respect to the experimental results, the effective radiative efficiency is noticeably lower for the thickest sample of 1500 nm, which is again due to its longer radiative lifetime. Note that the drop in signal beyond 10^7 W/m^2 is hypothesized to be a result of Auger recombination [1], since conduction band filling and leakage over the barrier (~260 meV) are not significant in GaInP lattice matched to GaAs. However, it is possible that a

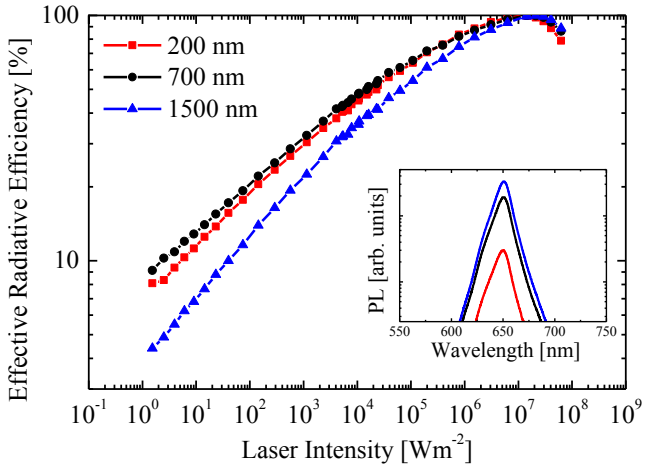

Figure 5. Effective radiative efficiency using power-dependent relative photoluminescence as a function of incident 532 nm laser intensity. Inset plot shows the PL of each sample under the highest injection level.

TABLE I
Effective Radiative Recombination Coefficient and Low-Level Injection Lifetime for All Three GaInP-DHs

DH Thickness [nm]	DH Doping [cm^{-3}]	B_{RAD} [cm^{3}s^{-1}]	τ_{RAD} [ns]
200	1×10^{17}	2.28×10^{-10}	44
700	1×10^{17}	1.19×10^{-10}	88
1500	1×10^{17}	0.669×10^{-10}	168

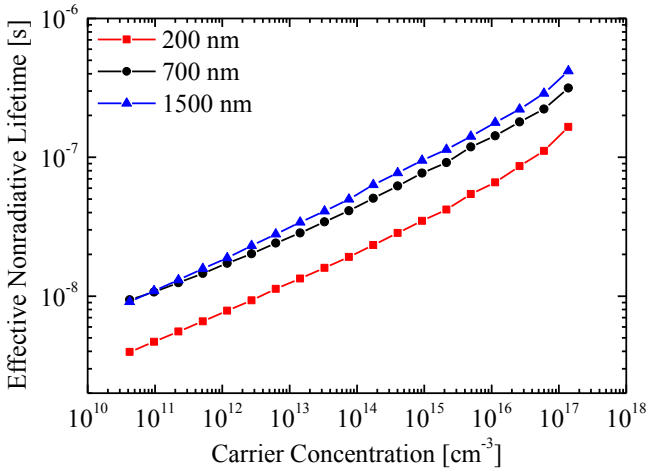

Figure 6. The extracted effective nonradiative lifetime (including interface recombination) as a function of excess carrier concentration using the power-dependent relative photoluminescence measurements from Figure 5 combined with the theory discussed in [1].

fraction of carriers in the Γ-band are scattered into the indirect L-band of GaInP (~157 meV [15]), whereby spontaneous emission becomes significantly less probable. These errors could amount to ~1% of the reported effective SRH lifetimes.

B. Nonradiative Lifetime Extraction

The effective nonradiative lifetime is extracted as a function of injection level using the method described in Ref. 1, and illustrated in Figure 6 for the set of GaInP DHs. The thinnest structure clearly has the shortest nonradiative lifetime, which is primarily due to interface recombination. The thicker two samples, 700 and 1500 nm, demonstrate similar lifetimes throughout the entire range of injection levels within uncertainties, which indicates that surface recombination is less important. Note that the nonradiative lifetime is plotted as a function of carrier concentration rather than laser intensity due to the dependence of carrier concentration on DH thickness. Also note that, based on the model described in Ref. 1, calculating the carrier concentration requires a number of assumptions regarding the steady-state carrier dynamics within the DH, such as carrier homogeneity throughout the DH and reaching a purely radiative system under high injection. These considerations, including other uncertainties such as in the incident laser beam diameter and the high signal to noise ratio under low injection, all result in considerable uncertainty in the calculated excess carrier concentration.

The remaining unknown is the magnitude of the surface recombination velocity, which can be extracted by exploiting equation (4); note that equation (4) assumes the SRV is the same for both barrier interfaces, which may not be the case due to surface pinning at the ARC/AlGaInP interface. For an excess carrier concentration comparable to 1 sun of ~4×10^{12} cm^{-3}, the inverse lifetime is plotted as a function of inverse thickness in Figure 7a. These results can be compared to the results in Figure 4. A surface recombination velocity of 700±50 cm/s, which is in reasonable agreement with that extracted from the EQE-based results from section III. The

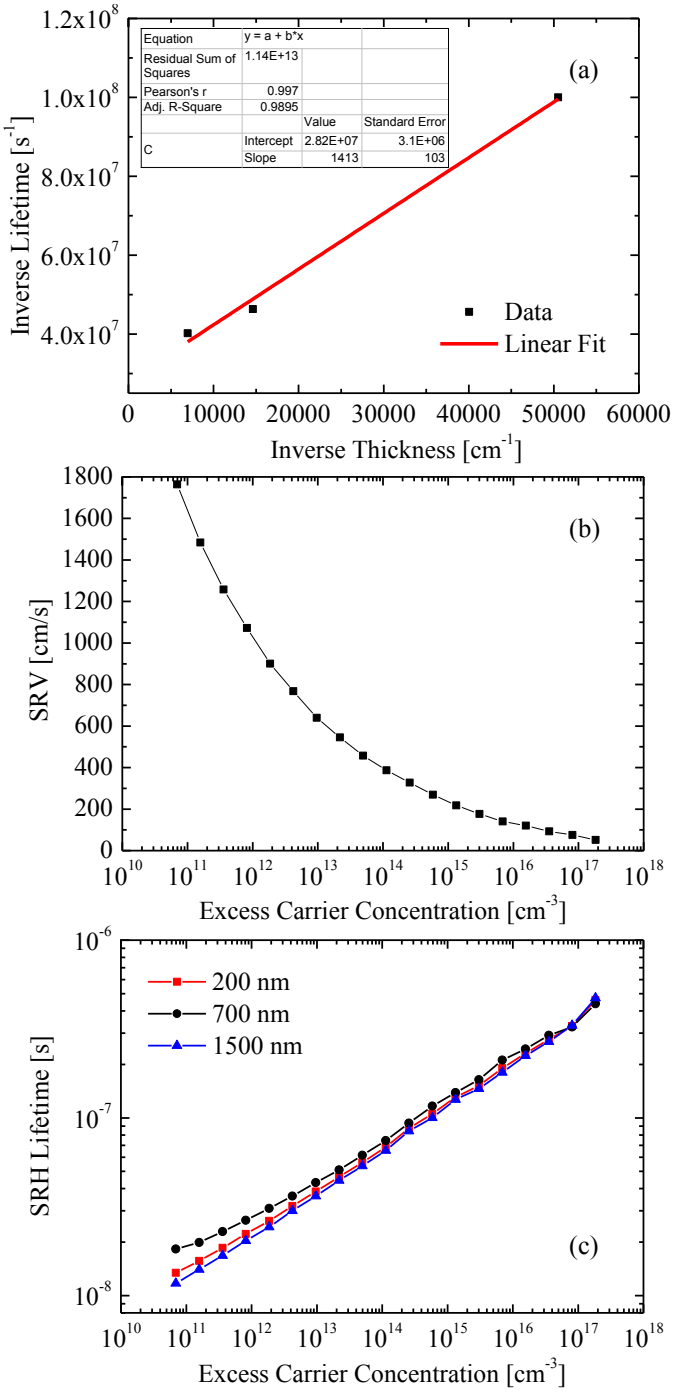

Figure 7. a) Inverse effective nonradiative lifetime as a function of inverse sample thickness for an injection close to 1 sun (~4e12 cm^{-3}), b) extracted surface recombination velocity (SRV) at the AlGaInP/GaInP interface as a function of excess carrier concentration, and b) corrected bulk SRH lifetime as a function of excess carrier concentration after removing the influence of SRV.

bulk SRH lifetime extracted from Figure 7a is (35±4) ns, and is also in agreement with the bulk SRH lifetime extracted from Figure 4 of (47±11) ns. According to Figure 7a , the 700 and 1500 nm thick samples show similar effective nonradiative lifetimes, whereas the thinnest structure shows a significantly shorter lifetime. Both observations are in agreement with

Figure 4. Interestingly, the extracted effective nonradiative lifetimes using the PDR-PL method are consistently shorter than the EQE-modeling method. This can be attributed to some extent to the uncertainty in the probed excess carrier concentrations in the three samples for the EQE measurement. Another source of uncertainty is the chosen AlGaInP/GaInP barrier, which has a strong impact on the carrier dynamics in the simulation. Lastly, it is important to note the calculated excess carrier concentration in the PDR-PL method is difficult to accurately evaluate. Overall, however, both methods produce results in agreement with each other for the same samples within their respective uncertainties, thus demonstrating the validity of both methods.

The extracted SRV parameters are illustrated in Figure 7b as a function of injection level. The general trend of decreasing surface recombination velocity from 1800 cm/s to <50 cm/s with increasing carrier concentration is explained by the saturation of traps at the interfaces. Finally, the SRH lifetime for the GaInP absorber can be extracted using equation (4) in combination with the results of Figure 6 and Figure 7b, which are shown in Figure 7c. Overall, the SRH lifetime shows little variation between the samples as a function of carrier concentration. The small variation observed under low injection may originate from a number of different factors, including the slight variation in reactor quality from run to run, the measurement uncertainty (which leads to uncertainty in the extracted SRV and the SRH lifetime), the assumption of electron hole population homogeneity in the samples as a function of injection, and the signal to noise ratio of the PL under low injection. As the excess carrier concentration increases, one can observe that the SRH lifetime approaches up to 0.5 μs; note that values extracted for a purely radiative state are not shown here, since the SRH lifetime goes to infinity. These nonradiative lifetimes are comparable to high-injection lifetime values of GaAs [1], which demonstrates both high material quality and a strong injection dependence of the defects in *p*-type GaInP. Interestingly, no SRH lifetime saturation is observed for low injection in the samples studied here, in contrast to that observed for GaAs [1].

V. Conclusions

In conclusion, the luminescence coupling of a GaInP DH stacked on a GaAs *p-n* junction was investigated quantitatively using modeling and simulation to extract the nonradiative recombination lifetime of disordered GaInP. The modeling methodology accounts for photon recycling and luminescence coupling, and produces consistent results for similar samples. For the particular samples studied here, the bulk SRH lifetime was extracted as 47±11 ns under low injection of 4×10^{12} cm^{-3}, equivalent to approximately 1 sun. The SRH lifetime is found to increase as a function of increasing injection level according to bias light intensity dependent EQE measurements and power-dependent relative PL measurements, a sign that SRH traps are being saturated as a function of injection. The surface recombination velocity between GaInP and AlGaInP was estimated to be ~700 cm/s for the same injection level of 4×10^{12} cm^{-3}, and also decreases as a function of increasing injection level. The method of extracting the SRH lifetime using the proposed device modeling method is consistent with the power-dependent relative photoluminescence measurements. This demonstrates the accuracy and robustness of both methodologies. This technique can be applied to any double-heterostructure stacked on an active *p-n* junction.

Acknowledgements

This work has received funding from the European Union's Horizon 2020 research and innovation programme within the project CPVMatch under grant agreement No. 640873.

[1] Walker, A.W., Heckelmann, S., Karcher, C., Höhn, O., Went, C., Lackner, D., and Bett, A., W., *Nonradiative parameter extraction using intensity-dependent photoluminescence of III-V semiconductor double-heterostructures.* Journal of Applied Physics, **119**(155702), p. 1-10, 2016.

[2] R. K. Ahrenkiel, B. M. Keyes, and D. J. Dunlavy, *Intensity-dependent minority-carrier lifetime in III-V semiconductors due to saturation of recombination centers*, Journal of Applied Physics, 70, 225, 1991.

[3] Lush, G.B., MacMillan, H.F., Keyes, B.M., Levi, D.H., Melloch, M.R., Ahrenkiel, R.K., and Lunstrom, M.S., *A study of minority carrier lifetime versus doping concentration in n- type GaAs grown by metalorganic chemical vapor deposition.* Journal of Applied Physics, **72**(4), p. 1436-42, 1992.

[4] Lush, G.B., Melloch, M.R., Lundstrom, M.S., Levi, D.H., Ahrenkiel, R.K., and MacMillan, H.F., *Microsecond lifetimes and low interface recombination velocities in moderately doped n-GaAs thin films.* Applied Physics Letters, **61**(20), p. 2440-2, 1992.

[5] Steiner, M.A., Geisz, J.F., Garcia, I., Friedman, D.J., Duda, A., and Kurtz, S.R., *Optical enhancement of the open-circuit voltage in high quality GaAs solar cells.* Journal of Applied Physics, **113**(12), p. 123109, 2013.

[6] Asbeck, P., *Self-absorption effects on the radiative lifetime in GaAs-GaAlAs double heterostructures.* Journal of Applied Physics, **48**(2), p. 820-22, 1977.

[7] Lumb, M.P., Steiner, M.A., Geisz, J.F., and Walters, R.J., *Incorporating photon recycling into the analytical drift-diffusion model of high efficiency solar cells.* Journal of Applied Physics, **116**(194504), 2014.

[8] Braun, A., Katz, E.A., Feuermann, D., Kayes, B.M., and Gordon, J.M., *Photovoltaic performance enhancement by external recycling of photon emission.* Energy & Environmental Science, **6**(5), p. 1499, 2013.

[9] Kayes, B.M., Nie, H., Twist, R., Spruytte, S.G., Reinhardt, F., Kizilyalli, I.G., and Higashi, G.S. *27.6% conversion efficiency, a new record for single-junction solar cells under 1 sun illumination*. in *37th IEEE Photovoltaic Specialists Conference*. Seattle, Washington, USA, 000004-8, 2011.

[10] Kosten, E.D., Kayes, B.M., and Atwater, H.A., *Experimental demonstration of enhanced photon*

recycling in angle-restricted GaAs solar cells. Energy & Environmental Science, **7**(6), p. 1907, 2014.

[11] Geisz, J.F., Steiner, M.A., Garcia, I., Kurtz, S.R., and Friedman, D.J., *Enhanced external radiative efficiency for 20.8% efficient single-junction GaInP solar cells.* Applied Physics Letters, **103**(4), p. 041118 (5 pp.), 2013.

[12] Dimroth, F., Grave, M., Beutel, P., Fiedeler, U., Karcher, C., Tibbits, T.N.D., Oliva, E., Siefer, G., Schachtner, M., Wekkeli, A., Bett, A.W., Krause, R., Piccin, M., Blanc, N., Drazek, C., Guiot, E., Ghyselen, B., Salvetat, T., Tauzin, A., Signamarcheix, T., Dobrich, A., Hannappel, T., and Schwarzburg, K., *Wafer bonded four-junction GaInP/GaAs//GaInAsP/GaInAs concentrator solar cells with 44.7% efficiency.* Progress in Photovoltaics: Research and Applications, **22**(3), p. 277-82, 2014.

[13] Walker, A.W., Höhn, O., Micha, D.N., Dimroth, F., and Bett, A., W., *Impact of Photon Recycling on GaAs Solar Cells Designs.* IEEE Journal of Photovoltaics, **5**(6), p. 1-10, 2015.

[14] Walker, A.W., Höhn, O., Micha, D.N., Wagner, L., Helmers, H., Dimroth, F., and Bett, A., W., *Impact of photon recycling and luminescence coupling on III–V single and dual junction photovoltaic devices.* Journal of Photonics for Energy, **5**(1), p. 053087, 2015.

[15] Walker, A., *Bandgap engineering of multi-junction solar cells using nanostructures for enhanced performance under concentrated illumination*, in *Physics*. 2013, University of Ottawa: Ottawa.

[16] Vurgaftman, I., Meyer, J.R., and Ram-Mohan, L.R., *Band parameters for III-V compound semiconductors and their alloys.* Journal of Applied Physics, **89**(11), p. 5815-75, 2001.

[17] Levinshtein, M., Rumyantsev, S., and Shur, M., eds. *Ternary and Quaternary III-V Compounds*. Handbook Series on Semiconductor Parameters. Vol. 2. 1999, World Scientific Publishing: Singapore. 205.

[18] Nelson, J., *The Physics of Solar Cells*. London: Imperial College Press, 2003.

[19] Höhn, O., Kraus, T., Schwarz, U.T., and Bläsi, B. *The Photonic Solar Cell - System Design and Efficiency Estimations*. in Proc. SPIE 9140, *Photonics for Solar Energy Systems V*. Brussels, Belgium, 91400B, 2014.

[20] Fetzer, C. M., Lee, R. T., Stringfellow, G. B., Liu, X. Q., Sasaki, A., and Ohno, N. *Effect of surfactant Sb on carrier lifetime in GaInP epilayers*, Journal of Applied Physics, **91**(1), 199-203, 2002.